Global and Planetary Change 64 (2008) 3–15

Contents lists available at ScienceDirect

Global and Planetary Change

journal homepage: www.elsevier.com/locate/gloplacha

Possible impacts of 21st century climate on vegetation in Central and West Africa

Christine Delire *, Alfred Ngomanda [1], Dominique Jolly [2]

Paléoenvironnements, Institut des Sciences de l'Evolution, Université de Montpellier, cc 61, place E. Bataillon, Montpellier, 34095 France

ARTICLE INFO

Article history:
Received 11 August 2006
Accepted 13 January 2007
Available online 26 August 2008

Keywords:
vegetation model
climate change
Central and West Africa

ABSTRACT

We evaluate the possible effects of climate change on vegetation in Central and West Africa. We chose two climate scenarios from the IPCC Third Assessment Report, ECHAM3 with scenario B2 and HADCM3 model with scenario A1FI, to force the dynamic vegetation model IBIS. Both climate scenarios are warmer everywhere in the domain, wetter around Lake Chad and drier along the Atlantic coast. We chose not to consider the physiological effect of increased CO_2 on plant production and kept CO_2 fixed at 350 ppmv. Our simulations of the end of the 21st century result in less extensive tropical forests and reduced leaf area index and net primary productivity (NPP) where forest remains. At the northern and southern limits of the forest there is also a switch between tropical evergreen types and tropical deciduous types. With one climate scenario, vegetation cover and NPP increase around Lake Chad. The simulated climate change also results in widespread increase in evapotranspiration and reduction in runoff and NPP (proxies for important ecosystem services, like freshwater availability, food, timber and fuel supply) along the Atlantic coast. Additional simulations where only one variable is changed show that temperature, through its effect on evapotranspiration and NPP plays a crucial role in vegetation change in the region.

© 2008 Elsevier B.V. All rights reserved.

1. Introduction

According to the Inter-governmental Panel on Climate Change (IPCC), Africa as a whole is highly vulnerable to climate change (IPCC, 2001a,b). This region is home to a fast growing population (240 million for West Africa, 800 million for the entire continent in 2000), and a very large diversity of ecosystems ranging from tropical evergreen forests to savannas, grasslands and desert. The diverse climate regimes associated with these ecosystems are subject to large inter-annual, inter-decadal and multi-decadal variations, particularly with regard to precipitation (Hulme et al., 2001; Nicholson, 2001). Africa also has a very sparse observational network (IPCC, 2001a,b). Therefore, climate change and its impacts on ecosystems and water resources are particularly difficult to predict. The potential role of land cover change on regional climate further complicates this task.

There is a growing number of simulations of the 21st century by ocean–atmosphere general circulation models (AOGCMs). All models simulate temperature increases over Africa but the amplitude of the warming depends on the model and the socio-economic scenario used. There is much less agreement on the simulated precipitation changes. Joubert and Hewitson (1997) and the IPCC (2001b) report suggest that precipitation might increase over much of the interior of the African continent. Further analysis shows that this result might not be robust. First, the magnitude of the change is not large in comparison to the precipitation variability (observed and simulated, see Ruosteenoja et al., 2003) leading to results that are not statistically significant. Second, most current AOGCMs are unable to simulate the magnitude of the inter-decadal precipitation variability that has been observed (Hulme et al., 2001). In a multi-model study of the 20th century simulations of Sahel drought from the 1970s to1990s, Lau et al. (2006) showed that half of the models are not able to reproduce the drought and that those that do are not able to reproduce its timing and duration. Hence, AOGCMs probably don't capture all the processes responsible for this low frequency variability. Recently, Neelin et al. (2006) compared the precipitation simulated by 10 AOGCMs following IPCC's SRES A2 scenario. They show a drying trend in the tropics, especially in the Gulf of Mexico and central America, but little model agreement in terms of precipitation change in Africa for June–July–August, the wet season in the Sahel (see Neelin et al., 2006, Fig. 8). Most models simulate precipitation increases somewhere in the Sahel with decreases along the Gulf of Guinea, but 2 models result in the opposite pattern. Temperature changes simulated by AOGCMs for the 21st century are much more robust and the signal is larger than the internal variability (Ruosteenoja et al., 2003).

With the exception of S. Africa, there are very few studies of the impacts of future climate change on vegetation in Africa. Cao et al. (2001) studied changes in the carbon cycle of African ecosystems due to climate change. Hély et al. (2006) used a dynamic vegetation model

* Corresponding author. Now at Groupe d'etude de l'atmosphere meteorologique, CNRS-Meteo-France, 42 av Coriolis, 31057 Toulouse, France.
E-mail address: christine.delire@univ-montp2.fr (C. Delire).
[1] Now at Institut de Recherche en Ecologie tropicale, BP: 13354 Libreville-Gabon.
[2] Deceased.

0921-8181/$ – see front matter © 2008 Elsevier B.V. All rights reserved.
doi:10.1016/j.gloplacha.2008.01.008

to study the sensitivity of biomes to theoretical changes in precipitation regimes and focused in particular to changes in seasonality. Africa also appears in the global modeling study of vegetation shifts due to climate change of Neilson et al. (1998) and in the recent modeling study aimed at evaluating the risk of climate-induced changes in key ecosystem processes (Scholze et al., 2006).

We know however from paleoenvironmental data that vegetation in Central and West-Africa can experience large shifts. Around 5500 yr before present, the climate of the Sahara abruptly switched from the wet conditions that prevailed during the early to mid-Holocene to the present desert conditions. Less humid conditions led to important shifts in structure and composition of African lowland rainforest during the late Holocene (Vincens et al., 1999; Ngomanda et al., 2007). Pollen data from the central part of Gabon revealed concurrent major changes in the lake-levels and rainforest dynamics over the past 1500 yr. The northern hemisphere "Medieval Warm Period" (~1100–800 cal yr BP) was characterized by decadal-scale fluctuations of lake-levels coinciding with the opening and persistence of canopy gaps in the mature forest cover. During the Little Ice Age (500–200 BP), lake-levels were low, tropical rainforest cover decreased and composition shifted from evergreen species to more deciduous ones (Ngomanda et al., 2007). In the 20th century, a shift in forest species was also observed in the West African Sahel (Gonzales, 2001).

Here, we use a dynamic vegetation model, forced with AOGCM output, to examine the impact of climate change on vegetation in Central and West Africa. We run our dynamic vegetation model with the results of two different AOGCMs and two different scenarios giving contrasting climate results over Central and West Africa. Because of the uncertainty in precipitation, we chose not to limit our study to the effect of rainfall changes on vegetation but include all the available GCM simulated variables: rainfall, temperature, cloudiness, humidity, and wind speed. We then separately analyze the influence of rainfall and temperature on vegetation changes.

2. IBIS-2: model description

In this study, we use an updated version of the Integrated Biosphere Simulator (IBIS2.6), a process-based dynamic global ecosystem model (Foley et al., 1996; Kucharik et al., 2000). IBIS (version 2) is a comprehensive model of terrestrial biospheric processes, and includes land-surface physics, canopy physiology, plant phenology, vegetation dynamics and competition, and carbon cycling.

The IBIS land-surface module is based on Thompson and Pollard's (1995a,b) LSX model and simulates the energy, water, carbon, and momentum balance of the soil-vegetation–atmosphere system on an hourly timestep. The module includes two vegetation layers (i.e., "trees" and "grasses and shrubs") and six soil layers to simulate soil temperature, soil water, and soil ice content over a total depth of 4 m. Physiologically-based formulations of C3 and C4 photosynthesis, stomatal conductance (Farquhar et al., 1980; Collatz et al., 1991, 1992), and respiration (Amthor, 1984) are used to simulate canopy gas exchange processes. This approach provides a mechanistic link between the exchange of energy, water, and CO_2 between vegetation canopies and the atmosphere. Budburst and senescence depend on climatic factors following the empirical algorithm presented by Botta et al. (2000).

IBIS represents vegetation in 12 plant functional types (PFT) that differ in their form (trees, shrubs, grasses), leaf type (broadleaf or needleleaf), patterns of leaf display (evergreen or deciduous), and photosynthetic pathway (C3 or C4). The 12 PFTs compete for light and water and their relative abundance in each gridcell is based on the annual carbon balance. For example, where trees and grasses coexist, trees are able to capture light first but the rooting profile of grasses gives them first access to water as it infiltrates through the soil. In drought conditions, grasses will be favored, trees will accumulate less carbon, will grow fewer leaves and eventually die. Competition between grass types or between tree types results from differences in carbon allocation, phenology, leaf type, or photosynthetic pathway.

For this study of Central and West Africa where wildfires play an important role, we added the Thonicke et al. (2001) fire module to IBIS. This fire module was originally developed for the LPJ dynamical vegetation model (Sitch et al., 2003) and needed few adjustments to work within the framework of IBIS. The simulated wildfires in Central and West Africa tend to favor savannas at the expense of tropical deciduous forests (Delire et al., in preparation).

The standard input data to IBIS are a global soil texture dataset (Global Soil Data Task Group, 2000) and monthly averaged values of temperature, precipitation, relative humidity, cloudiness, temperature range, wind speed, and number of rainy days from Climate Research Unit's dataset (Mitchell and Jones, 2005). IBIS then uses a stochastic weather generator to infer the hourly data needed for the land-surface module.

IBIS has been extensively tested against site-specific biophysical measurements (Delire and Foley, 1999; El Maayar et al., 2001; Kucharik et al., 2006) as well as spatially extensive ecological (Kucharik et al., 2000) and hydrological data (Lenters et al., 2000; Coe et al., 2002).

3. Simulation design

We ran two sets of IBIS simulations: 1) to simulate the natural vegetation in the 20th century using observed climate data, b) to simulate the vegetation at the end of the 21st century, using results from two different climate models forced with two different IPCC Third Assessment Special Report on Emissions Scenarios (SRES) (Nakicenovic et al., 2000). We chose the HADCM3 model (Johns et al., 2003) with scenario A1FI and the ECHAM4 model (Roeckner et al., 1999) with scenario B2a. The HADCM3 atmospheric horizontal resolution is 2.5°×3.75° and the ECHAM4 atmospheric horizontal resolution is 2.8125°×2.7673°. Both sets of IBIS simulations were performed on a 0.5° longitude by 0.5° latitude spatial grid using the same soil texture data set (Global Soils Data Task Group, 2000) and interpolating the climate data as explained later. The study was conducted between 5.5°S and 16°N, and 17.5°W and 18°E.

We chose not to consider the physiological effect of increased CO_2 on plant production and kept the CO_2 atmospheric concentration constant at 350 ppmv for both sets of simulations. Increased CO_2 levels tend to favor carbon assimilation by directly enhancing photosynthesis and improving water-use efficiency. It thus affects both ecosystem functioning and structure. This so-called CO_2 fertilization effect is well established in young-stand temperate forests (Norby et al., 2005). But there are very few data on the effect of higher CO_2 levels in mature forests, especially in tropical regions (Norby et al., 2005). There are no free-air CO_2 enrichment (FACE) experiments in tropical forests for instance, although these ecosystems represent 50% of the terrestrial biomass (Ainsworth and Long, 2005). Also, there are few data in sub-tropical arid and semi-arid environment. Inverse modeling studies of the carbon sources and sinks during the 1980s and 1990s indicate that natural ecosystems in the tropics from 30 N to 30 S took up anthropogenic CO_2 counterbalancing the deforestation carbon flux. But there is no consensus on whether this uptake of carbon is due to CO_2 fertilization effect (Prentice et al., 2001). If it were to be true in the tropics, it could have very large effects. Jolly and Haxeltine (1997) for instance showed with the BIOME model that low atmospheric CO_2 alone during the last glacial maximum 21 000 yr ago could explain the large vegetation changes in tropical African montane vegetation deduced from pollen data. IBIS, like most dynamical global vegetation models (DGVM) does not incorporate the effect of nutrient limitation (like nitrogen) on assimilation because of the lack of data and scientific consensus. This version of IBIS, like many other DGVMs, also doesn't include the photosynthetic downregulation under high

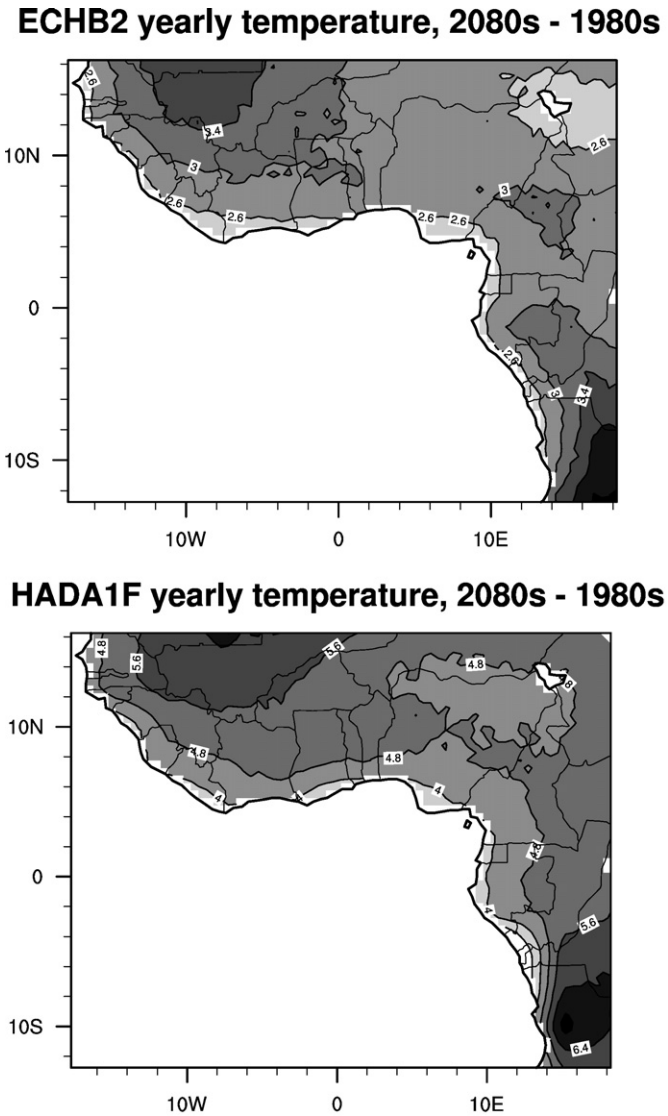

Fig. 1. Difference between annual mean temperature for the 2080s and the 1980s as simulated by a) the ECHAM model with scenario B2 (ECHB2) b) the HADCM3 model with scenario A1FI (HADA1F), interpolated at the 0.5° resolution. The time averages are taken from 2070 to 2099 for the 2080s and 1961 to 1990 for the 1980s. Contours are displayed every 0.2 °C from 2.4 °C for ECHB2 and every 0.8 °C from 3.2 to 7.2 °C for HADA1F.

ambient CO_2 concentration that occur in some plant species (Sharkey, 1985). In a recent modeling study, El Maayar et al. (2006) showed that neglecting this downregulation effect significantly bias predictions of net primary productivity under high CO_2 concentration, mainly in the mid to high latitude. Therefore, like Higgins (2007) we preferred to maintain CO_2 concentration constant at the value used in IBIS validation (350 ppmv).

The model is first spun up for 200 yr with the 1961–1990 climatology of monthly average temperature, precipitation, relative humidity, cloudiness, wind speed, temperature range and number of rainy days compiled by New et al. (1999). From there, the model is run for the 20th century with the 1901–2000 time-series of the same variables from the CRU TS2.1 dataset (Mitchell and Jones, 2005).

The 21st century climate was determined from the AOGCM's monthly mean anomalies and the observed climate variability from the 20th century. The monthly mean temperature, precipitation, humidity, radiation and wind speed simulated by the AOGCMs were first interpolated at the 0.5° resolution using bilinear interpolation. The monthly mean climatology for 2070–2099 was then computed as the sum of the observed climatology for 1961–1990 and the difference between the mean interpolated AOGCM output for 2070–2099 and for 1961–1990. The observed variability from the 1901–2000 CRU TS2.1 dataset was then imposed on the monthly mean climatology for the 2070–2099. Using the simulated anomalies is preferred than using the direct GCM output to avoid well-recognized errors in the mean climate simulated by AOGCMs. Moreover the climatic forcing at the end of the 21st century has the same inter-annual variability and the same trend as the climate of the 20th century given by the CRU TS2.1 dataset. We could use the changes in climate variability simulated by the two AOGCMs. In Africa however, and more precisely in the Sahel, inter-annual variability of the precipitation depends most likely on the interaction of the ocean, the vegetation and the atmosphere (Zeng et al., 1999; Nicholson, 2000; Wang and Eltahir, 2000). The GCMs used in the SRES phase don't simulate vegetation dynamics and none are able to reproduce the long-term evolution of the precipitation over the Sahel during the 20th century (Lau et al., 2006). We therefore chose to use the observed 20th century inter-annual variability thereby neglecting the likely changes in climate variability.

We use the results of the 200-year spin-up run of IBIS with the present-day climatology as initial conditions for the 21st century runs. We then run IBIS for 200 yr with the 21st century climate forcing described above and analyze the results of the last 50 yr and compare

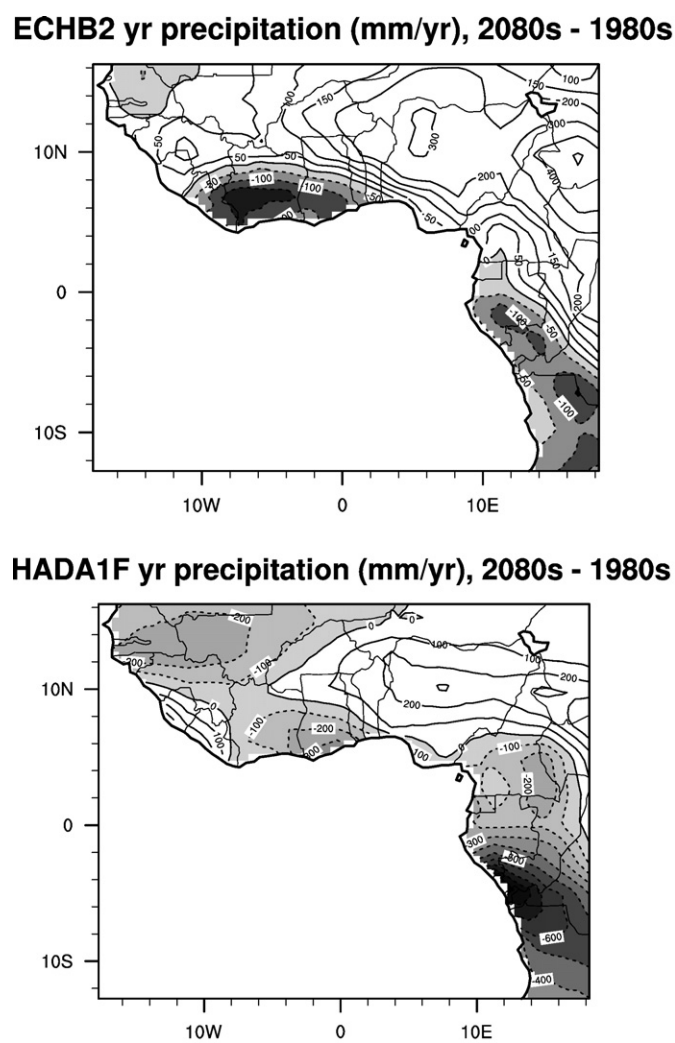

Fig. 2. Same as Fig. 1 but for annual precipitation. Gray = decrease, White = increase. Contours are displayed every 50 mm/yr from −150 to 450 mm/yr for ECHB2 and every 100 mm/yr from −800 to 300 mm/yr for HADA1F.

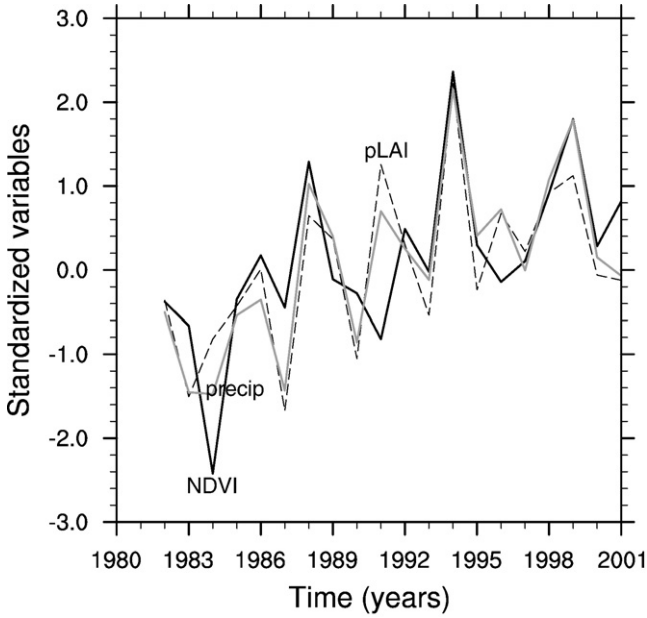

Fig. 3. Standardized value of satellite-derived peak-season NDVI (from Hickler et al., 2005), annual precipitation from the CRU TS2.1 dataset (Mitchell and Jones, 2005), and modeled peak-season leaf area index (pLAI), averaged over the Sahel [12W–35E, 10N–16N].

them to the last 50 yr of the present-day IBIS run. Our results are near equilibrium results for the vegetation.

4. Climate scenarios

The IPCC Third Assessment Report Scenarios (SRES TAR) A1FI and B2 are at the opposite ends in terms of socio-economic development assumptions (Nakicenovic et al., 2000). Scenario A1FI describes a future world of very rapid economic growth relying on fossil-fuels while Scenario B2 describes a future where local development and sustainability are a concern (Nakicenovic et al., 2000). The resulting CO_2 concentration by 2100 reaches about 600 ppmv in the case of scenario B2 and 925 ppmv for A1FI. A detailed description of all the greenhouse gas concentrations, ozone, sulfur and sulfate aerosols input to the HADCM3 model is given in Johns et al. (2003). The resulting change in total radiative forcing at the tropopause in 2100 relative to 1900 is much higher for scenario A1FI (7.9 W m^{-2}) than for B2 (5.3 W m^{-2}) in the case of the HADCM3 model (Johns et al., 2003). In terms of global temperature change, scenario B2 results in global temperature increases between 2 and 3.5 °C, while scenario A1FI produces global temperature increases between 3 and 6 °C, depending on the climate model (IPCC, 2001a).

Here, we use the results of the HADCM3 model with scenario A1FI (Johns et al., 2003) and the results of ECHAM4/OPYC (Roeckner et al., 1999) to force our vegetation model and simulate the impact of these climate changes on the vegetation in West Africa. We chose these two climate scenarios because one results in a very large climate change signal over Africa (the HADCM3 model with A1FI) and the other in a more moderate "average" climate change (the ECHAM model with scenario B2).

The temperature increase simulated by ECHAM4/OPYC with scenario B2 (here and after ECHB2) over West Africa is between 2 and 4 °C, with most of the regions experiencing increases of about 2 to 3 °C (Fig. 1a). With HADCM3 under scenario A1FI (HADA1F), the warming is more intense, above 4 °C for most regions and reaching 7 °C in the south of the domain (Fig. 1b). The spatial pattern of heating is rather similar for both models, with maximums in the northwest and south of the domain, and minimums around Lake Chad.

The seasonality of the precipitation in the region is linked to the migration of the inter tropical convergence zone (ITCZ). North of about 9°N, the climate is marked by one wet season peaking in August and one dry season from November to March. Around the equator, there are two wet seasons, one peaking in March–April and the other in October–November, separated by two drier seasons, the short dry season in December and the dry season from June to September.

Most of the precipitation changes according to ECHB2 occur in June, July, and August (JJA) with a drying along the Atlantic and increases inland between 10 and 12°N in the Sahel (Fig. 2). With HADA1F, precipitation changes are more dramatic, with a strong decrease in precipitation during the November wet season and during the short dry season in December, January and February (DJF). In boreal summer, the pattern of change is similar in HADA1F and ECHB2, with precipitation increases centered south of Lake Chad and decreases elsewhere. The amplitude of the decrease is bigger with HADA1F than with ECHB2. According to Johns et al. (2003), this JJA increase in precipitation in the HadCM3 model is due to a northward shift of the ITCZ associated with the greater warming of the Northern Hemisphere displacing the thermal equator northward. A similar northward move of the ITCZ was obtained with another AGCM forced by HADCM3 SSTs (Caminade et al., 2006). The pattern of precipitation change with ECHB2 (positive anomalies N of the ITCZ on the tropical oceans and negative anomalies S, not shown) suggests a similar explanation. Chou and Neelin (2004) and Chou et al. (2006) attribute this result to a general pattern of increasing precipitation in convective zones and drying at its margins. Due to the high inter-annual variability of precipitation in the region, the GCM simulated precipitation changes are not necessarily statistically significant (see Ruosteenoja et al., 2003). In their study of 10 AOGCMs, Neelin et al., (2006) showed that there is little model agreement in the exact location of the precipitation changes for the 2080s in this region of Africa for June–July–August (Neelin et al., 2006, Fig. 7). However, most models simulate a statistically significant increase in precipitation somewhere around Lake Chad and decrease along the Atlantic coast.

5. Simulated vegetation

5.1. Present-day

Before discussing the simulated vegetation changes, we briefly examine how well IBIS simulates 20th century vegetation in West Africa. Recently, using the Normalized Difference Vegetation Index (NDVI) derived from satellite measurements, Eklundh and Olsson (2003) showed that vegetation greenness increased in the Sahel region from 1982 to 1998. Hickler et al. (2005) used the LPJ dynamical global vegetation model (Sitch et al., 2003) forced by the CRU dataset (New et al., 2000) to show that climatic changes and mainly precipitation changes are the major driver for this greening trend. We obtain a similar result with IBIS (Fig. 3).

The version of IBIS used here only simulates natural vegetation (Fig. 4a). To compare with a map of present-day vegetation, we use Ramankutty and Foley's (1998) map of fractional crop cover at the 0.5° resolution to mask out agricultural land. Each gridcell where the cropland fraction is larger than 0.1 is mapped as a mosaic between crop and forest or crop and grassland according to the original IBIS simulated vegetation type in the gridcell (Fig. 4b). We compare the corrected simulated vegetation with the GLC2000 vegetation of Africa map (Mayaux et al., 2003). IBIS effectively represents the gradient from the equator to the tropic, simulating tropical evergreen forest and woodland around the equator, deciduous forests at the northern and southern limits of the evergreen forest, and further north, savannas, grassland, shrubland and desert. There are differences however. Compared with the GLC2000 vegetation map, IBIS correctly simulates the vegetation in 65% of the area. IBIS tends to overestimate the forest cover, mainly north of about 4°N and south of 4°S (Fig. 4).

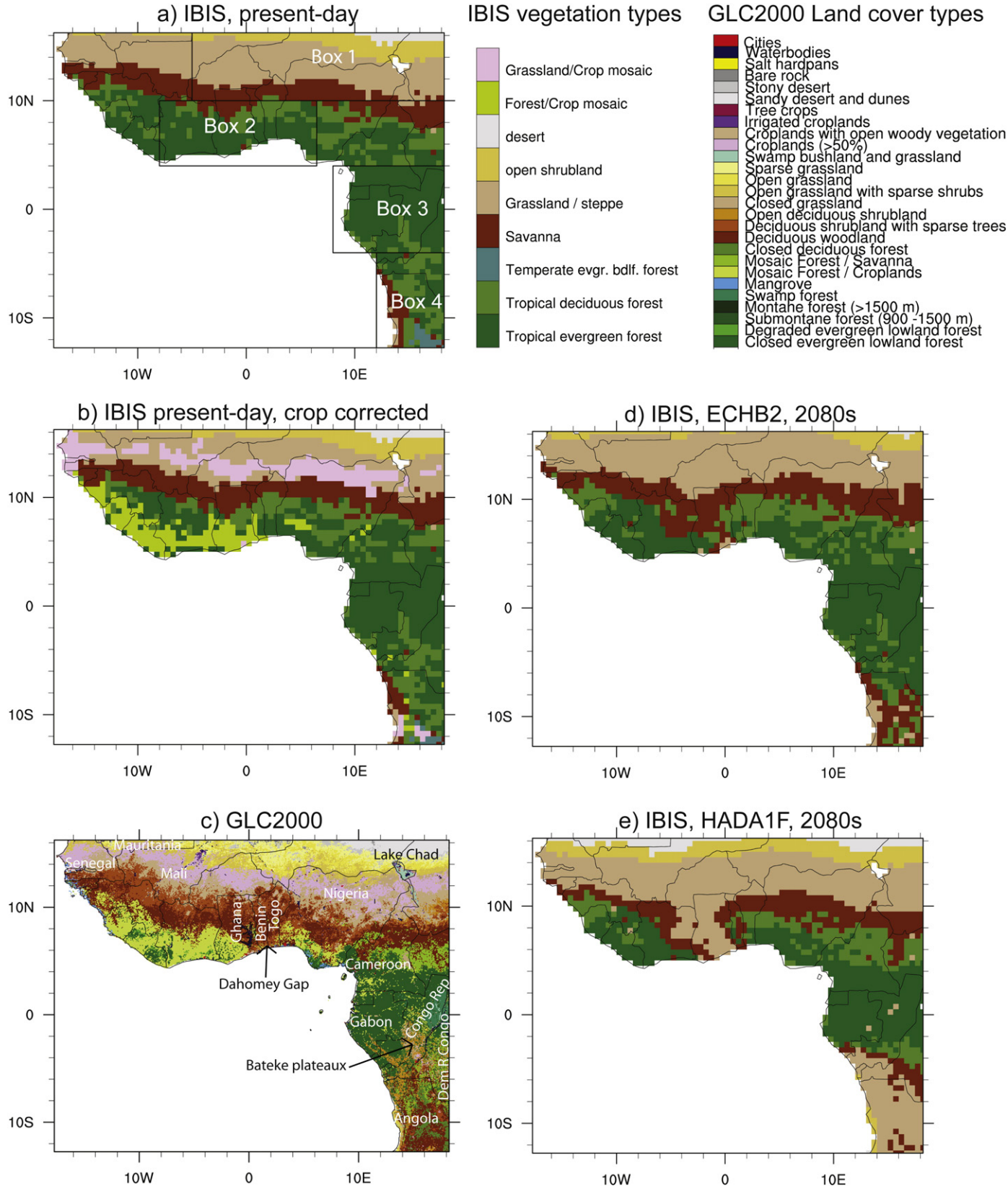

Fig. 4. Simulated and observed distribution of vegetation/land cover types a) simulated by IBIS forced with the present-day CRU TS2.1 climate, b) same as a) but corrected by Ramankutty and Foley (1998) cropland dataset c) derived from satellite observations (Global Land Cover 2000—GLC200, Mayaux et al., 2003), d) simulated by IBIS forced with the ECHB2 anomalies for the end of the 21st century, e) simulated by IBIS forced with the HADA1F anomalies for the end of the 21st century. 4 c) In white: country names cited in the text, in black: geographic features cited in the text.

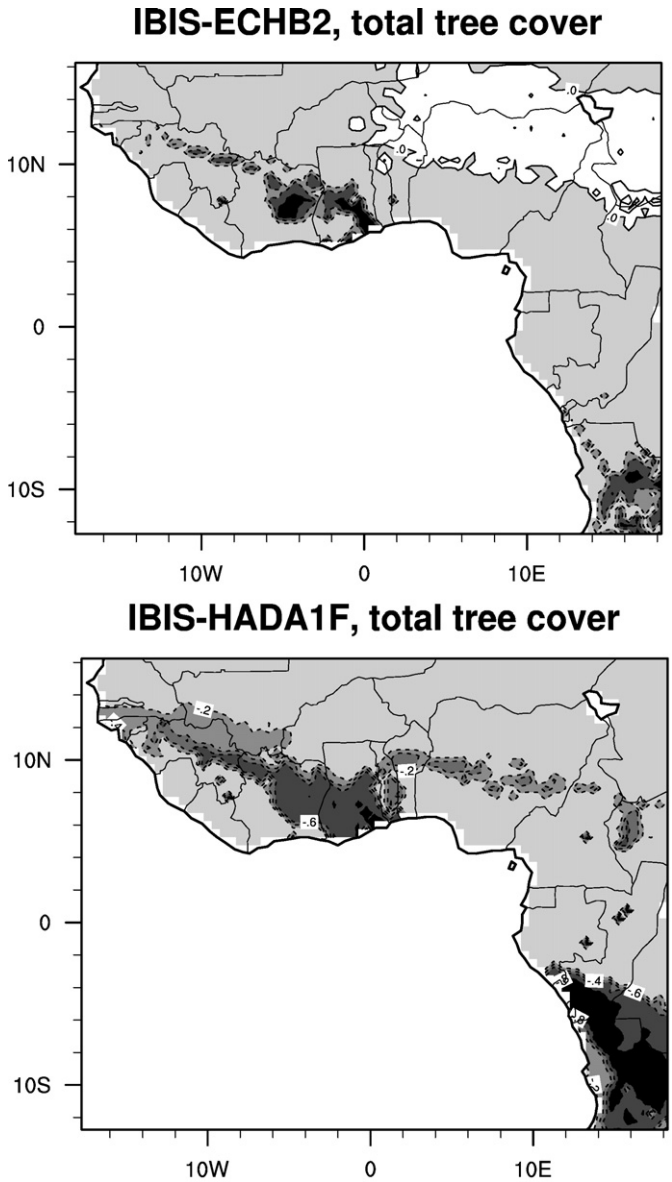

Fig. 5. Difference in fractional tree cover between the end of the 21st and 20th centuries simulated by IBIS a) forced with the ECHB2 anomalies b) forced with the HADA1F anomalies. Gray = decrease, White = increase. Contours are displayed every 0.2 from −0.6 to 0.4 (−60 % to+40%) for ECHB2 and every 0.2 from −0.8 to 0 (−80% to 0%) for HADA1F.

The so-called "Dahomey Gap" in Ghana, Togo and Benin, for instance, is not well represented by the model. IBIS forced with 20th century climate data simulates a closed canopy forest in the region (tropical evergreen and deciduous forest); in reality, observed tree cover doesn't exceed 40% and the forest canopy is open. Paleo-evidence has shown that vegetation cover in this region of Africa has changed substantially during the last 20 000 yr. During the mid-Holocene, closed canopy forest covered the whole region but was replaced with open savannas by 5000 BP (Salzmann and Hoelzmann, 2005). Since then, the landscape has remained open. Similarly, forest cover is too extensive in N Cameroon, and Angola. In S–E Gabon and Congo, the model fails to simulate the vast open expanse of grassland called the "Bateke Plateaux" (around 2°S, 15°E).

The overestimation of forest cover in some regions could be due to limitations of the model (IBIS does not include nitrogen or phosphorus limitations for instance) or to the impact of disturbances not included in the model. According to Sankaran et al. (2005) African savannas receiving more than 650 mm/yr in annual mean precipitation are "unstable" systems under current climate conditions. 650 (±134) mm/yr seem sufficient for woody canopy closure and disturbances (fire, herbivory) are needed for the coexistence of tree and grasses. The regions where IBIS overestimates forest cover have annual mean precipitation well above this limit suggesting disturbances not included in the model (human activity, herbivory activity) are responsible for the open tree canopy. Thonicke's natural fire module used in IBIS might also not be accurate enough for this region. It is hard to determine the cause of the thinned forest in these regions. Is it purely the result of soil conditions and natural fire, or if it is linked to human activity (or both). It is known for instance that the Bateke Plateaux are systematically burned down every year by the local population (Schwartz et al., 1998), which prevents the development of a forest. On the other hand, the soils of the Bateke Plateaux are very poor (Laraque et al., 1998) and might not be properly represented in IBIS. As well, Ramankutty and Foley's cropland map does not include pasture or human-induced fires. It also underestimates crop cover in heavily populated Nigeria (Ramankutty, 2004). Hence human impact on vegetation is largely underestimated in Fig. 4b.

5.2. Vegetation changes

Both climate scenarios result in the same general pattern of decreased forest cover at the end of the 21st century compared to the present-day (Figs. 4d,e, 5 Table 1). The only exception is a slight increase around Lake Chad with ECHB2. In the northern hemisphere the limit between forest and savannas moves south, together with the limit between savannas and grasslands. The most striking feature is the wide opening of the Dahomey Gap in Benin and Togo. According to these two simulations, this region loses most of its tree cover and is exclusively covered by grassland by the end of the 21st century. The reduction in forest cover is much more drastic with the HADA1F scenario, in the Benin region but also in the southeast corner of the domain (Angola), where forest is replaced by savanna, grassland, and shrubland (Fig. 4).

The shrubland/desert limit is displaced further north with the ECHB2 simulation north of Lake Chad, and further south around Mali, Mauritania and Senegal with HADA1F. Both climate models simulate precipitation increases in the Lake Chad region, but the increase is

Table 1
Area covered by vegetation types, average NPP (net primary productivity) and LAI (leaf area index) of vegetation types as simulated by IBIS forced with present-day CRU TS2.1 dataset (control) and the ECHB2 and HADA1F climate anomalies for the 2080s

	Area (km^2)			NPP (kg C m^{-2} yr^{-1})			Total LAI		
Vegetation types	Control	ECHB2	HADA1F	Control	ECHB2	HADA1F	Control	ECHB2	HADA1F
Tropical evergreen forest/woodland	2.12	1.86	1.34	1.06	0.96	0.88	7.85	7.08	6.52
Tropical deciduous forest/woodland	0.96	0.91	0.65	0.91	0.76	0.69	6.7	5.62	5.07
Savanna	1.02	1.26	0.97	0.66	0.65	0.62	5.03	5.33	5.25
Grassland/steppe	1.49	1.81	2.27	0.3	0.32	0.33	2.06	2.26	2.61
Open shrubland	0.42	0.28	0.59	0.06	0.06	0.06	0.76	0.77	0.68
Desert	0.10	0.02	0.32	0.02	0.02	0.01	0.28	0.37	0.27

much more modest with HADA1F and not sufficient to sustain increased vegetation growth.

In addition to a reduction in forest cover associated with an increase in grassland and shrubland, the two climate scenarios also result in a shift between tropical evergreen PFTs and tropical deciduous PFTs at the outer limits of the tropical forest region (not shown).

Overall, in these two simulations, changes in NPP (Fig. 6, Table 1) and total LAI (Table 1) show that the remaining tropical forest is less productive, especially in southwest Africa, and most importantly Gabon, the Congo Republic and the Democratic Republic of the Congo. The increased precipitation in the interior of the continent explains why savannas and grassland are more productive in these simulations.

6. Changes in the hydrologic cycle

In the two climate scenarios chosen here, precipitation increases over a large region around, and south of, Lake Chad and decreases elsewhere (Fig. 2). Evapotranspiration does not follow this pattern and increases over a much larger area including most of the tropical forest region for both scenarios. Some of the increase is linked to increased rainfall, particularly in water-limited areas such as the Sahel. But evapotranspiration increases around the equator (Gabon) where the precipitation decreases. Even where evapotranspiration decreases, the ratio of evapotranspiration over precipitation sometimes increases (Fig. 7). Evapotranspiration depends not only on soil moisture availability (hence rainfall), but also on the available energy at the surface, wind speed and atmospheric humidity. Changes in temperature, humidity, wind speed and radiation play an important role in AET (actual evapotranspiration). The effect of increased temperature on AET is further investigated with additional simulations in Section 8.

Runoff changes follow mostly the same pattern as rainfall changes: increases around Lake Chad and decreases elsewhere. Because of the evapotranspiration increases however, the area with reduced runoff is larger than that with reduced rainfall (Fig. 7).

The reduced rainfall and increased evapotranspiration in the tropical forest lead to reduced runoff that might strongly affect the coastal rivers. Box 3 for instance (see Fig. 4a) which includes Gabon has a reduction of yearly runoff of 5% (in ECHB2) to 55% (in HADA1F). This runoff reduction was also found by Arnell (2004) in his comparison of the runoff simulated by 6 different GCMs following IPCC's scenario A2. Four GCMs simulate widespread runoff decreases for 2050 around the Gulf of Guinea and the other two GCMs simulate more patchy decreases. Using the average rainfall changes of 6 GCMs, de Wit and Stankiewicz (2006) find decreased runoff south of the equator and in the Dahomey Gap, and increased runoff elsewhere around the Gulf of Guinea.

In their study of the risk of climate-induced changes in ecosystem processes during the 21st century, Scholtze et al. (2006) find a high probability of runoff decrease in West Africa north of the Gulf of Guinea together with a fair probability of runoff increase around Lake Chad. This risk analysis is based on the results of 52 GCM simulated climate scenarios forcing the LPJ dynamical global vegetation model. Contrary to our results, they find a fairly high probability of runoff increase in the equatorial regions. LPJ simulates runoff reductions in this region with only 5 of the 52 climate scenarios.

The two climate scenarios we chose do not modify fundamentally the shape of the seasonal cycle of precipitation, evapotranspiration and runoff (Fig. 8). In the Sahel region around Lake Chad (box 1), rainfall increases mainly during the wet season, and the simulated wet season starts 2 months early with ECHB2. This additional amount of water is partly evaporated and partly runs off. It also result in wetter soils. Wet season runoff is lower with ECHB2 despite higher rainfall. This is due to the increased vegetation cover (mostly C4 grasses and deciduous trees) in the region resulting in higher evapotranspiration rates. This increased vegetation cover is sustained by the longer wet season in comparison to the present and the HADA1F scenario.

The Dahomey Gap box (box 2) is interesting because a fairly moderate reduction in rainfall (5%) combined with increased evapotranspiration due to higher temperatures results in a reduction of about 40% in volumetric water content at the peak of the wet season (September).

Around the equator (box 3), rainfall increases with ECHB2 and decreases with HADA1F, mainly during the "October wet season". Evapotranspiration increases with both scenarios due to the temperature increase while runoff and soil water content decrease, much more so with HADA1F because of the rainfall decrease.

In Angola and Congo (box 4), both scenarios result in reduced precipitation but the decrease is much more important with HADA1F as is the number of months with no rainfall (4 in comparison to 2 in the present-day and with ECHB2). Contrary to the other four regions where evapotranspiration increased for both scenarios, it increases with ECHB2 and decreases in box 4 with HADA1F. The reduction in rainfall is such that the soil moisture content remains close to wilting point (0.370) during most of the year (June to February). Vegetation is

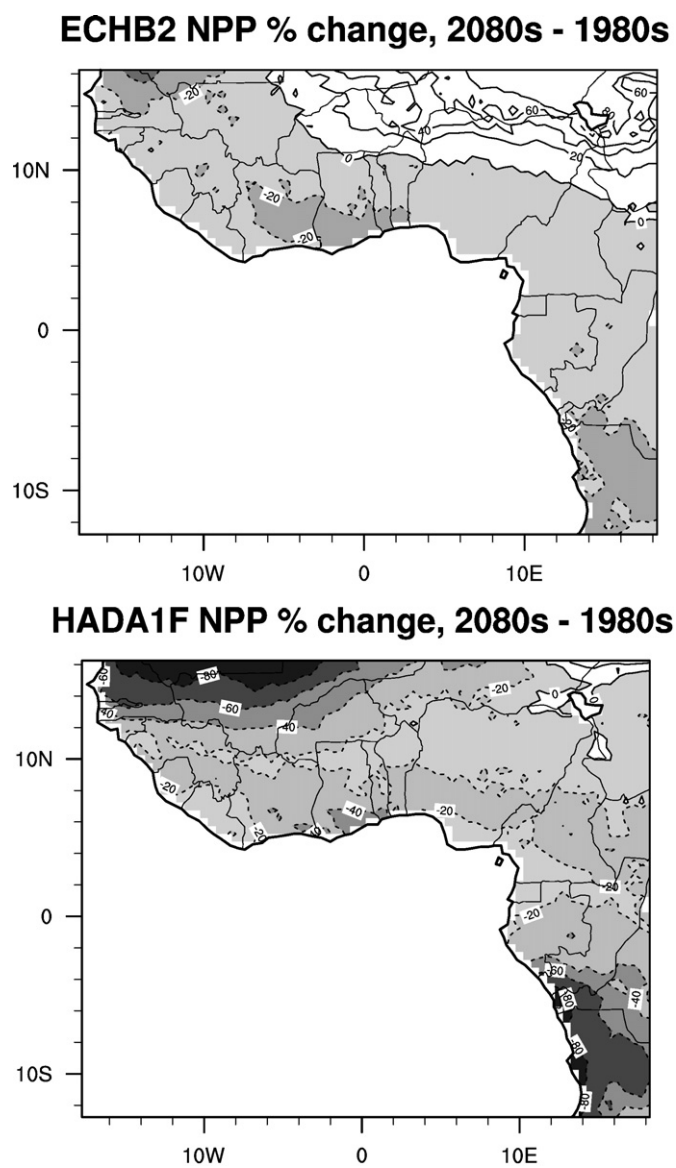

Fig. 6. Difference in NPP (net primary productivity) between the end of the 21st and 20th centuries simulated by IBIS a) forced with the ECHB2 anomalies b) forced with the HADA1F anomalies. Gray = decrease, White = increase. Contours are displayed every 0.1 kg C m^{-2} yr^{-1} from −0.4 to 0.2 kg C m^{-2} yr^{-1} for ECHB2 and every 0.1 kg C m^{-2} yr^{-1} from −0.8 to 0.1 kg C m^{-2} yr^{-1} for HADA1F.

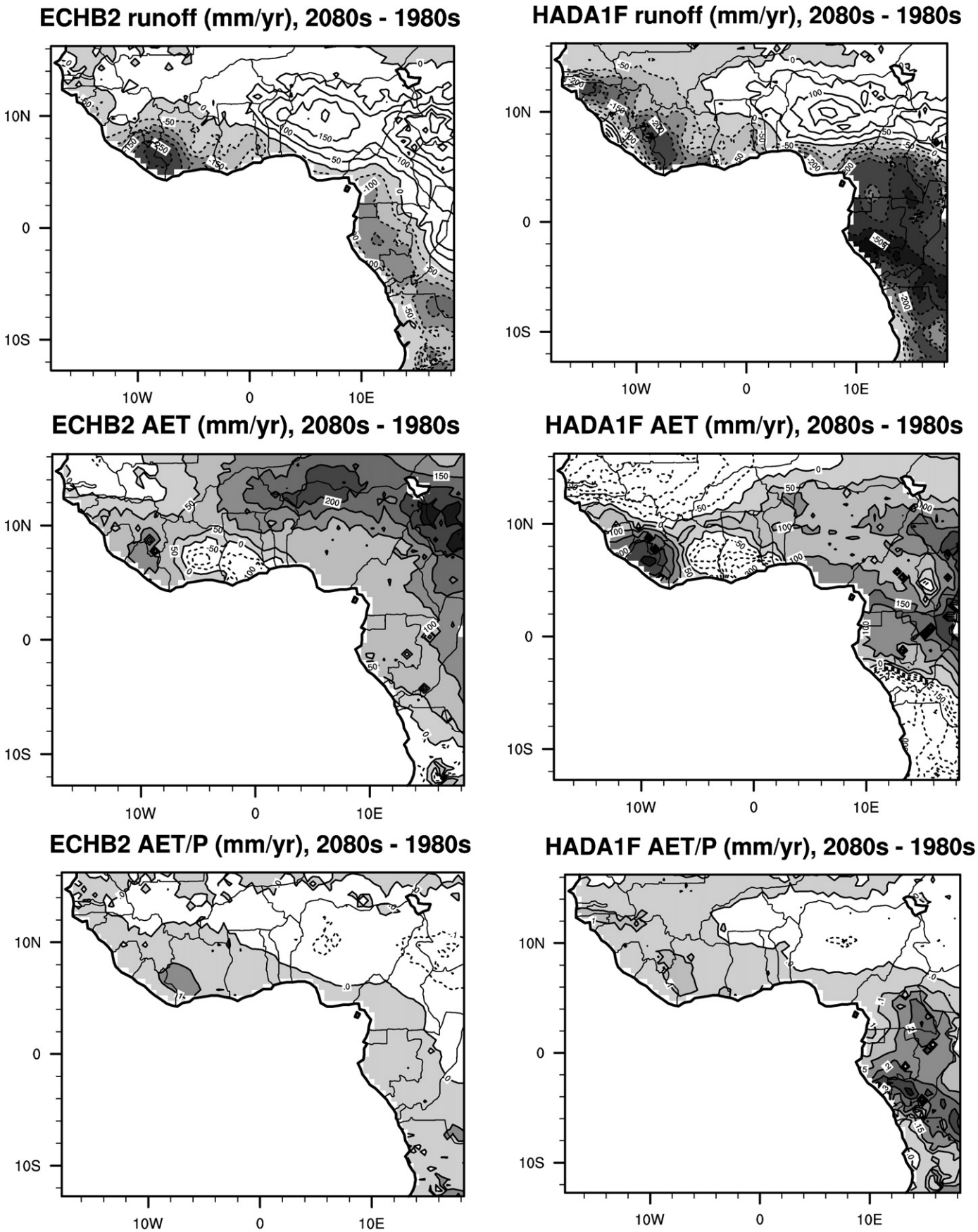

Fig. 7. Difference in total runoff, AET (actual evapotranspiration) and AET/P (ratio of evapotranspiration to precipitation) between the 2080s and the 1980s as simulated by IBIS forced with ECHB2 anomalies (column 1) and HADA1F (column 2). Gray = decrease and White = increase for runoff but Gray = increase and White = decrease for AET and AET/P.

highly water stressed, transpiration is strongly limited and soil evaporation increases do not compensate.

7. Changes in wildfire frequency

Thonicke's fire module coupled to IBIS simulates an increase in wildfire frequency (decrease in fire return interval) along the Atlantic coast with both climate scenarios (Fig. 9). This is due to the drier conditions linked to the decrease in precipitation and the increase in evapotranspiration. Wildfire frequency also increases around Lake Chad with the ECHB2 scenario because the wetter conditions enhance vegetation growth (Fig. 6) and availability of fuel for burning. Despite a similar increase in precipitation this doesn't happen with the HADA1F scenario. NPP only increases in a very small region N of Lake Chad and the increase is too small to give adequate fuel supply. Both scenarios result in a decrease in wildfire frequency in the continent interior but the location differ between the two scenarios: mostly in the Sahel with HADA1F and along a band just N of the tropical forest region with ECHB2. The pattern of increased and decreased wildfire frequency simulated with ECHB2 is similar to the pattern deduced by Scholtze

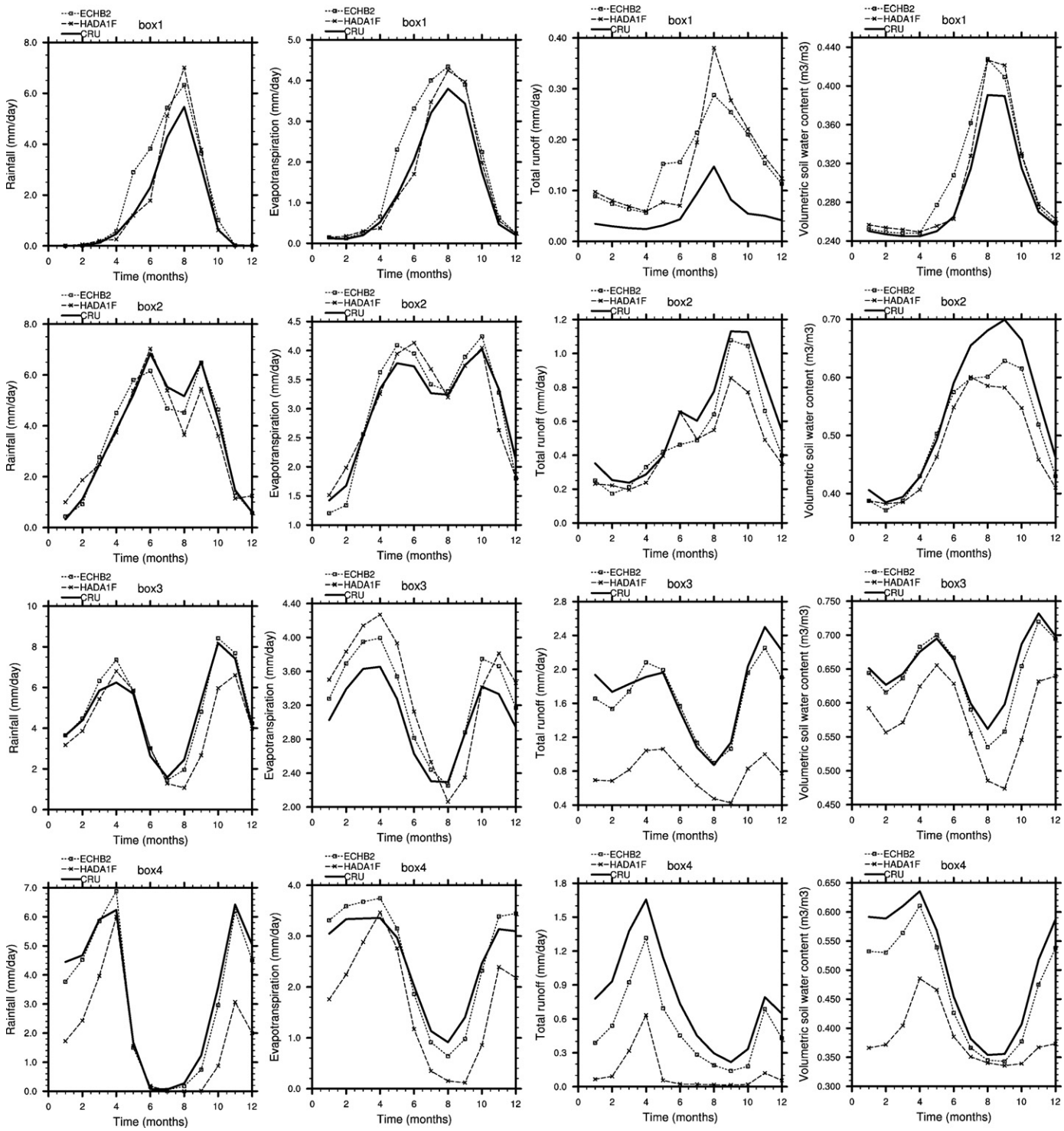

Fig. 8. Seasonal cycle of rainfall, evapotranspiration, total runoff and soil volumetric water content simulated by IBIS forced with the CRU TS2.0 dataset for the 20th century, the ECHB2 anomalies and the HADA1F anomalies for the 21st century. The 4 boxes are defined in Fig. 4a.

et al. (2006) for the GCMs that simulate a global temperature between 2 and 3 °C (ECHB2 simulates a global temperature increase of 2.5 °C). The decreased wildfire frequency in the Sahel following HADA1F scenario is only shared by two of the 16 scenarios that resulted in global temperatures higher than 3 °C in the Scholtze et al. (2006) study (HADA1F simulates a global temperature increase of 3 °C). In the equatorial regions where both ECHB2 and HADA1F result in increased frequencies, Scholtze et al. report either no significant change or a decrease. This is most likely linked with the high probability of runoff increase simulated by LPJ in the region.

8. Effect of precipitation, temperature

Impact studies of climate change in tropical areas often focus on precipitation changes, assuming these are the most important drivers of vegetation and hydrologic change. De Wit and Stankiewicz (2006) for instance only use the GCM simulated rainfall changes to infer the changes in river runoff. They do not take into account changes in temperature and/or evapotranspiration for instance. To test if precipitation change is indeed the most important driver of vegetation and hydrologic change in W-Africa, we performed additional simulations where one climate variable was changed according to the 2080s climate simulations but the others were kept fixed. The two variables chosen were precipitation and temperature. We call HADA1F-P (HADA1F-T) the simulation where all the forcing variables are from the 1961–1990 climatology except for the precipitation (temperature) taken from the HADA1F simulation of the 2080s as an anomaly. A similar experiment was done to test the importance of solar radiation changes only (HADA1F-S) but the effect is minor. This thought experiment allows us to determine if one change is more important.

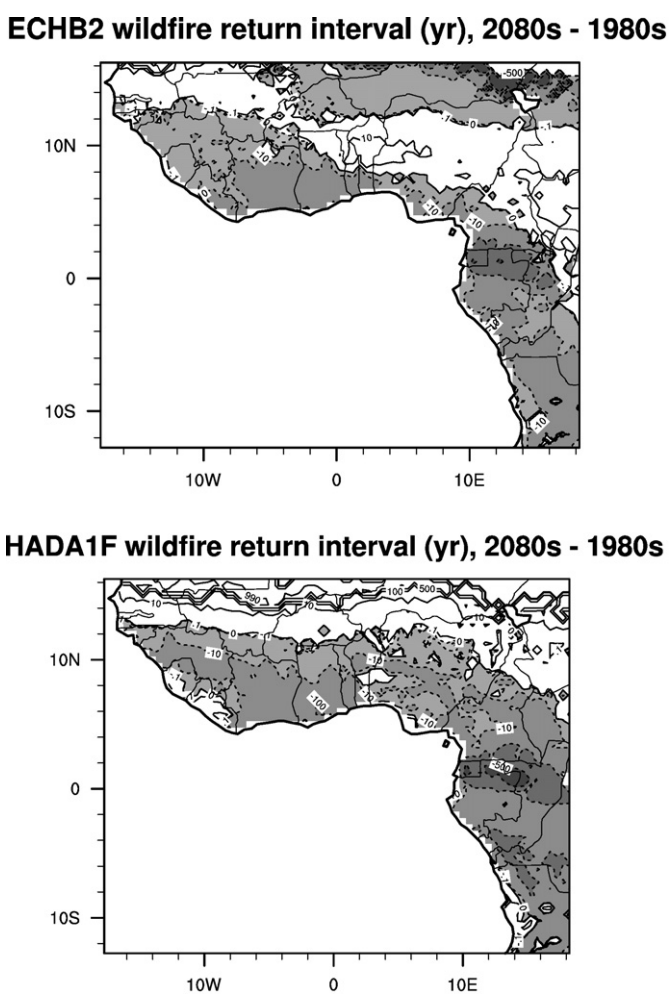

Fig. 9. Difference in wildfire return interval between the end of the 21st and 20th centuries simulated by IBIS a) forced with the ECHB2 anomalies b) forced with the HADA1F anomalies. Gray = decrease, White = increase. Contours are displayed for positive and negative differences in return interval of 990 yr, 500 yr, 100 yr, 10 yr, 0.1 yr, and 0 yr.

Table 2
Average yearly precipitation for each vegetation type from the present-day CRU TS2.1 dataset (control) and the ECHB2 and HADA1F climate anomalies for the 2080s and average yearly evapotranspiration (AET) for each vegetation type as simulated by IBIS forced with present-day CRU TS2.1 dataset (control) and the ECHB2 and HADA1F climate anomalies for the 2080s

	Precipitation (mm/yr)			AET (mm/yr)		
Vegetation types	Control	ECHB2	HADA1F	Control	ECHB2	HADA1F
Tropical evergreen forest/woodland	1686	1781	1748	1135	1221	1284
Tropical deciduous forest/woodland	1500	1617	1632	1070	1155	1228
Savanna	1080	1241	1267	928.3	1033	1067
Grassland/steppe	595	715	785	562.5	655.9	707.3
Open shrubland	252	299	281	248.4	289.6	276.8
Desert	127	215	175	127.2	219	175.8

To keep the simulations shorter we forced IBIS with the New et al. climatology of 1961–1990 for the present-day control simulation (Ctl_c) and with the differences in temperature (precipitation) from HADA1F between 2061–2090 and 1961–1990 added to the New et al. climatology. The use of present-day climatology as forcing to IBIS instead of the full time-series of the 20th century as in the three main simulations presented in section 4 results in small differences (compare results between Tables 2 and 3) that do not affect our conclusions.

Fig. 10 and Table 3 show the area covered by the different vegetation types in the temperature only simulation (HADA1F-T), precipitation only simulation (HADA1F-P) and with the full HADA1F climate scenario (HADA1F_c). Temperature changes only (HADA1F-T) result in variations in area that are larger than the variations from precipitation changes only (HADA1F-P) for the tropical evergreen forest, the grassland, shrubland and desert. Temperature changes (HADA1F-T) result in a reduction in area of the tropical evergreen forest that is 57% of the reduction simulated with the complete HADA1F_c climate scenario. In case of the HADA1F-P simulation, the reduction is only 49%. On the other hand, the HADA1F-P simulation has more impact on the area covered by tropical deciduous forest and savanna than the HADA1F-T simulation. This strong effect of temperature was also found by Higgins and Vellinga (2004) in their global scale study of ecosystem response to abrupt climate change, but only for tropical deciduous forests.

Temperature and precipitation have opposite effects on the area covered by savannas. Temperature changes (increases everywhere) result in a strong reduction in area mainly around 10°N (not shown) while precipitation changes result in savanna expansion (mainly S of Lake Chad where precipitation increases and in Angola where precipitation decreases). In the "Dahomey Gap", both temperature and precipitation independently reduce the forest cover but individually neither change is able to completely open the forest canopy as it is the case with the complete HADA1F climate scenario.

The sum of the effects of temperature changes alone (HADA1F-T) and precipitation changes alone (HADA1F-P) is not equivalent to the effect of the HADA1F_c climate scenario (hence the percentages do not add up to 100). Their relative importance depends on complex local conditions. Wind speed changes, radiation changes and humidity changes also play a role (minimal for radiation in this case).

Temperature and precipitation changes play competing roles in evapotranspiration changes, except for tropical deciduous forest and

Table 3
Area covered by vegetation types, average NPP (net primary productivity) and AET (actual evapotranspiration) of vegetation types as simulated by IBIS forced with present-day climatology of New et al. (1999) (control) and the ECHB2 and HADA1F climate anomalies for the 2080s

Vegetation types	Area ($\times 10^6$ km^2)				NPP (kg C m^{-2} yr^{-1})				AET (mm/yr)			
	Control	HADA1F	HADA1F_P	HADA1F_T	Control	HADA1F	HADA1F_P	HADA1F_T	Control	HADA1F	HADA1F_P	HADA1F_T
Tropical evg forest	2.131	1.408	1.916	1.724	1.088	0.887	1.060	0.887	1134.6	1281.8	1128.4	1289.8
Tropical dec forest	0.986	0.696	0.845	0.978	0.945	0.699	0.882	0.710	1069.0	1226.0	1079.9	1190.4
Savanna	0.924	0.915	1.125	0.765	0.681	0.578	0.643	0.608	950.9	1027.9	907.0	1062.9
Grassland/steppe	1.546	2.199	1.570	1.917	0.308	0.348	0.302	0.338	555.3	711.0	520.4	711.9
Open shrubland	0.390	0.514	0.489	0.510	0.059	0.055	0.058	0.053	235.8	261.4	210.4	292.1
Desert	0.128	0.405	0.179	0.268	0.018	0.015	0.019	0.016	129.1	163.0	134.3	170.3

desert (Table 3 and Fig. 10). Temperature changes (HADA1F-T) are responsible for increases in evapotranspiration while precipitation changes (HADA1F-P) result in decreased evapotranspiration for all the vegetation types except for the tropical deciduous forest and the desert. These two simulations clearly indicate that temperature changes are responsible for most of the evapotranspiration increases as mentioned in Section 6.

Changes in temperature alone (HADA1F-T) have a larger impact on net primary production (NPP) than changes in precipitation (HADA1F-P) (Table 3). The heating decreases NPP everywhere in the domain and for all vegetation types. This reduction is mostly due not only to an increase in wood and root respiration (directly dependant on temperature) but also to a reduction in gross primary production due to the reduced water availability following the increased evapotranspiration. As expected, patterns of NPP change follow rather closely the patterns of precipitation change in the precipitation changes only simulation (HADA1F-P). But the increases due to increased rainfall in the Sahel do not compensate for the decrease due to the rising temperature.

We repeated this series of additional simulations with the ECHB2 climate scenario. The results are qualitatively similar and show that temperature changes are a very important driver of vegetation and hydrologic change that cannot be neglected when studying climate change impact in this region.

9. Discussion–conclusion

The aim of this paper was to evaluate the possible effects of climate change on vegetation in West Africa, a particularly sensitive region of the world in terms of natural resources and biological conservation. We chose two climate models and economic scenarios to force the dynamic vegetation model IBIS; a particularly drastic climate scenario (HADA1F) and a “moderate” one (ECHB2). Both climate scenarios are warmer everywhere in the domain, wetter around Lake Chad and drier along the Atlantic coast. Our simulations of the end of the 21st century result in less extensive tropical forests and reduced LAI and NPP where forest remains. At the northern and southern limits of the forest there is also a switch between tropical evergreen types and tropical deciduous types. Vegetation cover and NPP increase around Lake Chad, mainly with the ECHB2 scenario. The simulated climate change also results in widespread increase in evapotranspiration and reduction in runoff and NPP along the Atlantic coast.

Additional simulations where only one variable was changed showed that temperature, through its effect on evapotranspiration and NPP plays a crucial role in vegetation change in the region. Higher temperatures result in increased evapotranspiration and decreased productivity. According to our simulations, studies of the impact of climate change on natural resources in this region must include all of

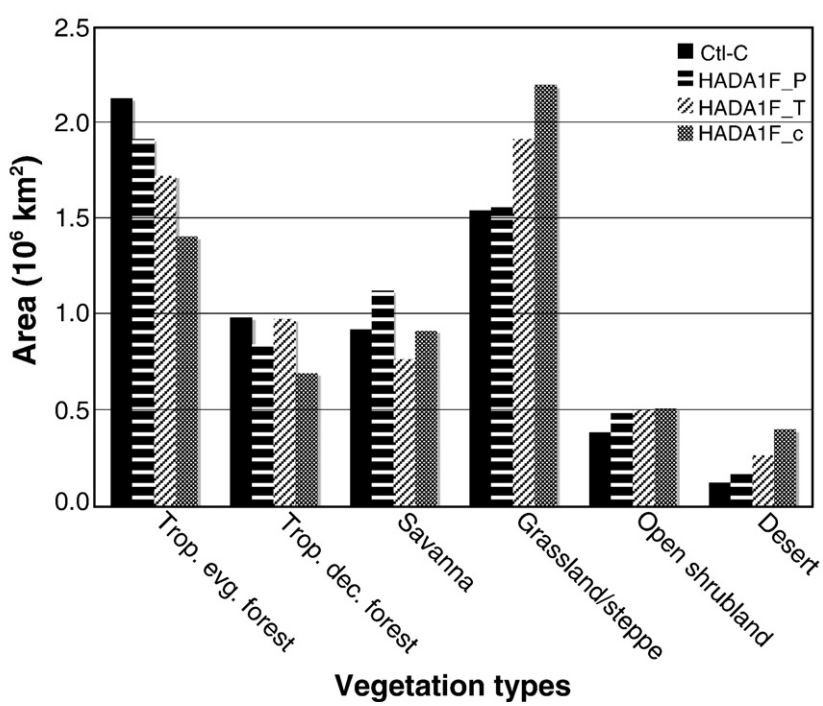

Fig. 10. Area covered by each vegetation types as simulated by IBIS forced with the present-day CRU climate (Ctlc_c), the HADA1F_P scenario, the HADA1F_T scenario and the HADA1F_c scenario. See text.

the GCM simulated variables, and in particular temperature (or evapotranspiration). For example, the reduction in river runoff simulated by de Wit and Stankiewicz (2006) is probably underestimated because they only considered rainfall changes. Similarly, studies aiming to evaluate crop yield and forest resources should account for the effects of temperature changes.

Our choice to fix the atmospheric CO_2 level at 350 ppmv tends to limit the scope of our conclusions. We chose to operate this way because there is almost no data on CO_2 fertilization effect in tropical ecosystems. If tropical ecosystems were to behave like young temperate forests, the increased CO_2 during the 21st century would enhance photosynthesis and increase water-use efficiency. This would counteract the effects of reduced precipitation and higher temperature on NPP and evapotranspiration and seriously modify the outcome. In Scholtze et al. (2006) for instance, simulations with the LPJ dynamical vegetation model taking into account the CO_2 fertilization effect result in a high probability of increased runoff in the equatorial regions. This opposite result is probably linked to the CO_2 fertilization effect.

We also did not take into account the human impact on vegetation. We only compared the natural vegetation (unperturbed by human activity) at the end of the 20th and 21st centuries. Current crop cultivation and grazing in the region strongly reduces forest extent and results in forest fragmentation (Fig. 4c). Current estimated deforestation rates are very high (the highest being Nigeria at 11% yr^{-1} between 2000 and 2005, according to the FAO) and according to the Integrated Model to Assess Global Environment (IMAGE, Alcamo et al., 1998) are expected to remain high at least until 2050. These would probably enhance the simulated reduction in forest cover and forest productivity due to climate change only.

Despite the uncertainty in the CO_2 fertilization effect in tropical ecosystems, it is likely that the future will be drier than today in large portions of northern and western Africa even if precipitation does increase modestly as some models suggest. Temperature changes are likely to drive a reduction in available water and exacerbate an already difficult situation. Similarly, temperature changes might result in a reduction of forest productivity that could hurt both forestry resources and biological conservation efforts as in Gabon for instance where 10% of the land-surface was recently set aside for conservation. Human-driven land-use changes not considered here will most likely enhance the reduction in forest cover and productivity.

Acknowledgements

We thank Michael Coe, Simon Donner and Navin Ramankutty for valuable discussion and useful comments on earlier drafts of this manuscript, and Michael Notaro for some of the graphics. We also thank Stephen Sitch and 2 anonymous reviewers for interesting questions and suggestions. We are grateful to the developers of the free software NCL used for the figures.

References

Ainsworth, E.A., Long, S.P., 2005. What have we learned from 15 years of free-air CO_2 enrichment (FACE)? A meta-analytic review of the responses of photosynthesis, canopy properties and plant production to rising CO_2. New Phytologist 165 (2), 351–371.

Alcamo, J., Leemans, R., Kreileman, E. (Eds.), 1998. Global Change Scenarios of the 21th Century. Pergamon, Elsevier Science Ltd., Oxford, UK (296 pp.).

Amthor, J.S., 1984. The role of maintenance respiration in plant growth. Plant, cell and environment 7 (561–569).

Arnell, N., 2004. Climate change and global water resources: SRES emissions and socio-economic scenarios. Global Environmental Change 14, 31–52.

Botta, A., Viovy, N., Ciais, P., Friedlingstein, P., Monfray, P., 2000. A global prognostic scheme of leaf onset using satellite data. Global Change Biology 6 (7), 709–725.

Caminade, C., Terray, L., Maisonnave, E., 2006. West African Monsoon System response to greenhouse gas and sulfate aerosols forcing under two emissions scenarios. Climate Dynamics 26 (5), 531–547.

Cao, M., Zhang, Q., Shugart, H.H., 2001. Dynamic responses of African ecosystem carbon cycling to climate change. Climate Research 17, 183–193.

Chou, C., Neelin, J.D., 2004. Mechanisms of global warming impacts on regional tropical precipitation. Journal Of Climate 17 (13), 2688–2701.

Chou, C., Neelin, J.D., Tu, J.Y., Chen, C.T., 2006. Regional tropical precipitation change mechanisms in ECHAM4/OPYC3 under global warming. Journal Of Climate 19 (17), 4207–4223.

Coe, M.T., Costa, M.H., Botta, A., Birkett, C.M., 2002. Long-term simulations of discharge and floods in the Amazon basin. Journal of Geophysical Research 107 (D20). doi:10.1029/2001JD000740.

Collatz, G.J., Ball, J.T., Grivet, C., Berry, J.A., 1991. Physiological and environmental-regulation of stomatal conductance, photosynthesis and transpiration — a model that includes a laminar boundary-layer. Agricultural and Forest Meteorology 54 (2–4), 107–136.

Collatz, G.J., Ribas-Carbo, M., Berry, J.A., 1992. Coupled photosynthesis–stomatal conductance model for leaves of C_4 plants. Australian Journal of Plant Physiology, 19, 519–538.

Delire, C., Foley, J.A., 1999. Evaluating the performance of a land surface/ecosystem model with biophysical measurements from contrasting environments. Journal of Geophysical Research 104 (D14), 16895–16909.

de Wit, M., Stankiewicz, J., 2006. Changes in surface water supply across Africa with predicted climate change. Science 311, 1917–1921.

Eklund, L., Olsson, L., 2003. Vegetation index trends for the African Sahel 1982–1999 vegetation index trends for the African Sahel 1982–1999. Geophysical Research Letters 30 (8) Art. No. 1430.

El Maayar, M., Price, D.T., Delire, C., Foley, J.A., Black, T.A., Bessemoulin, P., 2001. Validation of the Integrated Biosphere Simulator over Canadian deciduous and coniferous boreal forest stands. Journal of Geophysical Research 106 (D13), 14339–14355.

El Maayar, M., Ramankutty, N., Kucharik, C.J., 2006. Modeling global and regional net primary production under elevated atmospheric CO_2: on a potential source of uncertainty. Earth Interactions 10 Art. No. 2.

Farquhar, G.D., von Caemmerer, S., Berry, J.A., 1980. A biochemical model of photosynthetic CO_2 assimilation in leaves of C_3 species. Planta 149 (78–90).

Foley, J.A., Prentice, C.I., Ramankutty, N., Levis, S., Pollard, D., Sitch, S., Haxeltine, A., 1996. An integrated biosphere model of land surface processes, terrestrial carbon balance, and vegetation dynamics. Global Biogeochemical Cycles 10 (4), 603–628.

Global Soil Data Task Group, 2000. Global Soil Data Products CD-ROM (IGBP-DIS). Oak Ridge National Laboratory Distributed Active Archive Center, Oak Ridge, Tennessee, U.S.A. (http://www.daac.ornl.gov).

Gonzales, P., 2001. Desertification and a shift of forest species in the West African Sahel. Climate Research 17 (2), 217–228.

Hely, C., Bremond, L., Alleaume, S., Smith, B., Sykes, M.T., Guiot, J., 2006. Sensitivity of African biomes to changes in the precipitation regime. Global Ecology And Biogeography 15 (3), 258–270.

Hickler, T., Eklundh, L., Seaquist, J.W., Smith, B., Ardo, J., Olsson, L., Sykes, M.T., Sjostrom, M., 2005. Precipitation controls Sahel greening trend. Geophysical Research Letters 32 (21) Art. No. L21415.

Higgins, P.A.T., 2007. Biodiversity loss under existing land use and climate change: an illustration using northern South America. Global Ecology And Biogeography 16 (2), 197–204.

Higgins, P.A.T., Vellinga, M., 2004. Ecosystem responses to abrupt climate change: teleconnections, scale and the hydrological cycle. Climatic Change 64 (1–2), 127–142.

Hulme, M., Doherty, R., Ngara, T., New, M., Lister, D., 2001. African climate change: 1900–2100. Climate Research 17 (2), 154–168.

IPCC, Climate Change 2001a: The scientific basis. Contribution of Working Group I in The Third Assessment Report of the Intergovernmental Panel on Climate Change (eds Houghton JT, Ding Y, Griggs DJ, Noguer M, van der Linden PJ, Dai X, Maskell K, Johnson CA), Cambridge University Press, Cambridge, 881 pp.

IPCC, Climate Change 2001b: Impact, adaptation and vulnerability. Contribution of Working Group II in The Third Assessment Report of the Intergovernmental Panel on Climate Change (eds James J. McCarthy, O F Canziani, N A Leary, D J Dokken, K S White).

Johns, T.C., Gregory, J.M., Ingram, W.J., Johnson, C.E., Jones, A., Lowe, J.A., Mitchell, J.F.B., Roberts, D.L., Sexton, D.M.H., Stevenson, D.S., Tett, S.F.B., Woodage, M.J., 2003. Anthropogenic climate change for 1860 to 2100 simulated with the HadCM3 model under updated emissions scenarios. Climate Dynamics 20 (6), 583–612.

Jolly, D., Haxeltine, A., 1997. Effect of low glacial atmospheric CO_2 on tropical African montane vegetation. Science 276 (5313), 786–788.

Joubert, A.M., Hewitson, B.C., 1997. Simulating present and future climates of southern Africa using general circulation models. Progress In Physical Geography 21, 51–78.

Kucharik, C.J., Foley, J.A., Delire, C., Fisher, V.A., Coe, M.T., Lenters, J.D., Young-Molling, C., Ramankutty, N., Norman, J.M., Gower, S.T., 2000. Testing the performance of a Dynamic Global Ecosystem Model: water balance, carbon balance, and vegetation structure. Global Biogeochemical Cycles 14 (3), 795–825.

Kucharik, C., Barford, C., El Maayar, M., Wofsy, S.C., Monson, R.K., Baldocchi, D.D., 2006. A multiyear evaluation of a dynamic global vegetation model at three AmeriFlux forest sites: vegetation structure, phenology, soil temperature, and CO_2 and H_2O vapor exchange. Ecological Modelling 196, 1–31.

Laraque, A., Mietton, M., Olivry, J.C., Pandi, A., 1998. Influence des couvertures lithologiques et végétales sur les regimes et la qualité des eaux des affluents congolais du fleuve Congo. Revue des Sciences de l'Eau 11, 209–224.

Lau, K.M., Shen, S.S.P., Kim, K.M., Wang, H., 2006. A multimodel study of the twentieth-century simulations of Sahel drought from the 1970s to 1990s. Journal of geophysical research 111, D07111. doi:10.1029/2005JD006281.

Lenters, J.D., Coe, M.T., Foley, J.A., 2000. Surface water balance of the continental United States, 1963–1995: regional evaluation of a terrestrial biosphere model and the NCEP/NCAR reanalysis. Journal of Geophysical Research (Atmospheres) 105 (D17), 22,393–22,425.

Mayaux, P., Bartholomé, Massart, E.M., Van Cutsem, C., Cabral, A., Nonguierma, A., Diallo, O., Pretorius, C., Thompson, M., Cherlet, M., Pekel, J.F., Defourny, P., Vasconcelos, M.,

Di Gregorio, A., Fritz, S., De Grandi, G., Elvidge, C., Vogt, P., Belward, A., 2003. A land cover map of Africa. European Commission joint Research Center technical note. n EUR20665 EN.

Mitchell, T.D., Jones, P.D., 2005. An improved method of constructing a database of monthly climate observations and associated high-resolution grids. International Journal Of Climatology 25 (6), 693–712.

Nakicenovic, N., Alcamo, J., Davis, G., de Vries, B., Fenhann, J., Gaffin, S., Gregory, K., Grübler, A., Jung, T.Y., Kram, T., La Rovere, E.L., Michaelis, L., Mori, S., Morita, T., Pepper, W., Pitcher, H., Price, L., Raihi, K., Roehrl, A., Rogner, H.H., Sankovski, A., Schlesinger, M., Shukla, P., Smith, S., Swart, R., van Rooijen, S., Victor, N., Dadi, Z., 2000. IPCC Special Report on Emissions Scenarios. Cambridge University Press, Cambridge, United Kingdom. 599 pp.

Neelin, J.D., Munnich, M., Su, H., Meyerson, J.E., Holloway, C.E., 2006. Tropical drying trends in global warming models and observations. Proceedings of The National Academy of Sciences of The United States of America, 103, 16, pp. 6110–6115.

Neilson, R.P., Prentice, I.C., Smith, B., Kittel, T.G.F., Viner, D., 1998. Annex C. Simulated changes in vegetation distribution under global warming. In: Watson, R.T., Zinyowera, M.C., Moss, R.H. (Eds.), IPCC, Special Report on Regional Climate Impacts, pp. 439–456.

New, M., Hulme, M., Jones, P.D., 1999. Representing twentieth century space–time climate variability. Part 1: development of a 1961–90 mean monthly terrestrial climatology. Journal of Climate 12, 829–856.

New, M., Hulme, M., Jones, P.D., 2000. Representing twentieth century space-time climate variability. Part 2: development of 1901-96 monthly grids of terrestrial surface climate. Journal of Climate 13, 2217–2238.

Ngomanda, A., Jolly, D., Bentaleb, I., Chepstow-Lusty, A., Makaya, M., Maley, J., Fontugne, M., Oslisly, R., Rabenkogo, N., 2007. Lowland rainforest response to hydrological changes during the last 1500 years in Gabon, Western Equatorial Africa. Quaternary Research 67 (3), 411–425.

Nicholson, S., 2000. Land surface processes and Sahel climate. Reviews of Geophysics 38 (1), 117–139.

Nicholson, S.E., Grist, J.P., 2001. A conceptual model for understanding rainfall variability in the West African Sahel on interannual and interdecadal timescales. International Journal Of Climatology 21 (14), 1733–1757.

Norby, R.J., DeLucia, E.H., Gielen, B., Calfapietra, C., Giardina, C.P., King, J.S., Ledford, J., McCarthy, H.R., Moore, D.J.P., Ceulemans, R., De Angelis, P., Finzi, A.C., Karnosky, D.F., Kubiske, M.E., Lukac, M., Pregitzer, K.S., Scarascia-Mugnozza, G.E., Schlesinger, W.H., Oren, R., 2005. Forest response to elevated CO_2 is conserved across a broad range of productivity. Proceedings Of The National Academy Of Sciences Of The United States Of America 102 (50), 18052–18056.

Prentice, I.C., Farquhar, G.D., Fasham, M.J.R., Goulden, M.L., Heiman, M., Jaramillo, V.J., Kheshgi, H.S., Le Quéré, C., Scholes, R.J., Wallace, D.W.R., 2001. The carbon cycle and atmospheric carbon dioxide. In: Houghton, J.T., Ding, Y., Griggs, D.J., Noguer, M., van der Linden, P.J., Dai, X., Maskell, K., Johnson, C.A. (Eds.), IPCC, Climate Change 2001: The Scientific Basis. Cambridge University Press, Cambridge. 881 pp.

Ramankutty, N., 2004. Croplands in West Africa: a geographically explicit dataset for use in models. Earth Interactions, 8, 1–22.

Ramankutty, N., Foley, J.A., 1998. Characterizing patterns of global land use: an analysis of global croplands data. Global Biogeochemical Cycles 12 (4), 667–685.

Roeckner, E., Bengtsson, L., Feichter, J., Lelieveld, J., Rodhe, H., 1999. Transient climate change simulations with a coupled atmosphere–ocean GCM including the tropospheric sulfur cycle. Journal Of Climate 12 (10), 3004–3032.

Ruosteenoja, T.R., Carter, K., Jylhä, K., Tuomenvirta, H., 2003. Future climate in world regions: an intercomparison of model-based projections for the new IPCC emissions scenarios. The Finnish Environment 644. Finnish Environment Institute.

Salzmann, U., Hoelzmann, P., 2005. The Dahomey Gap: an abrupt climatically induced rain forest fragmentation in West Africa during the late Holocene. Holocene 15 (2), 190–199.

Sankaran, M., Hanan, N.P., Scholes, R.J., Ratnam, J., Augustine, D.J., Cade, B.S., Gignoux, J., Higgins, S.I., Le Roux, X., Ludwig, F., Ardo, J., Banyikwa, F., Bronn, A., Bucini, G., Caylor, K.K., Coughenour, M.B., Diouf, A., Ekaya, W., Feral, C.J., February, E.C., Frost, P.G.H., Hiernaux, P., Hrabar, H., Metzger, K.L., Prins, H.H.T., Ringrose, S., Sea, W., Tews, J., Worden, J., Zambatis, N., 2005. Determinants of woody cover in African savannas. Nature 438 (7069), 846–849.

Scholze, M., Knorr, W., Arnell, N.W., Prentice, I.C., 2006. A climate-change risk analysis for world ecosystems. Proceedings of the National Academy of Sciences of The United States of America 103 (35), 13116–13120.

Schwartz, D., Vincens, A., Elenga, H., Alexandre, A., Bertaux, J., Servant, M., Servant, S., Nguetsop, F., Bonvallot, J., Guillet, B., Mariotti, A., de Namur, C., Reynaud, I., Youta Happi, J., Delegue, M.A., Fuhr, M., 1998. Le Temps de l'Environnement, Editions du Mirail. Université de Toulouse-Le Mirail, Toulouse.

Sharkey, T.D., 1985. Photosynthesis in intact leaves of c-3 plants — physics, physiology and rate limitations. Botanical Review 51 (1), 53–105.

Sitch, S., Smith, B., Prentice, I.C., Arneth, A., Bondeau, A., Cramer, W., Kaplan, J.O., Levis, S., Lucht, W., Sykes, M.T., Thonicke, K., Venevsky, S., 2003. Evaluation of ecosystem dynamics, plant geography and terrestrial carbon cycling in the LPJ dynamic global vegetation model. Global Change Biology 9 (2), 161–185.

Thompson, S.L., Pollard, D., 1995a. A global climate model (genesis) with a land-surface transfer scheme (lsx). Part II: CO_2 sensitivity. Journal of Climate 8 (5), 1104–1121.

Thompson, S.L., Pollard, D., 1995b. A global climate model (GENESIS) with a land-surface-transfer scheme (LSX). Part 1: present-day climate. Journal of climate 8 (732–761).

Thonicke, K., Venevsky, V., Sitch, S., Cramer, W., 2001. The role of fire disturbance for global vegetation dynamics: coupling fire into a Dynamic Global Vegetation Model. Global Ecology & Biogeography 10 661–177.

Vincens, A., Schwartz, D., Elenga, H., Reynaud-Farrera, I., Alexandre, A., Bertaux, J., Mariotti, A., Martin, L., Meunier, J-D., Nguetsop, F., Servant, M., Servant-Vildary, S., Wirrmann, D., 1999. Forest response to climate changes in Atlantic Equatorial Africa during the last 4000 years BP and inheritance on the modern landscapes. Journal of Biogeography 26 (4), 879–885.

Wang, G.L., Eltahir, E.A.B., 2000. Role of vegetation dynamics in enhancing the low-frequency variability of the Sahel rainfall. Water Resources Research 36 (4), 1013–1021.

Zeng, N., Neelin, J.D., Lau, K.M., Tucker, C.J., 1999. Enhancement of interdecadal climate variability in the Sahel by vegetation interaction. Science 286 (5444), 1537–1540.